A *CTSG*

Relative expression (vs. *ACTB*)

n/d

βH3, ND HI, T2D HI, ND AC, T2D AC, BM

B *AMY2A*

Relative expression (vs. *ACTB*)

P=0.0005

n/d

βH3, ND HI, T2D HI, ND AC, T2D AC, BM

C *PDX1*

Relative expression (vs. *ACTB*)

P=0.0056
P=0.0031

n/d

βH3, ND HI, T2D HI, ND AC, T2D AC, BM

D *KRT19*

Relative expression (vs. *ACTB*)

P<0.0001

βH3, ND AC, T2D AC, Ducts

E *MUC1*

Relative expression (vs. ACTB)

P<0.0001

βH3, ND AC, T2D AC, Ducts

F

kDa

rhN-CELA3B   PE

1 2 5 10   1 2 5 10 (ng)

35 —
fl ▶
cl ▶

N-CELA3B

35 —
fl ▶
cl ▶

CELA3B

G

ND   T2D

5 µm

20 µm

INS   CELA3A   DAPI

H

N-CELA3B (islets)

ND
T2D

R²: 0.7810
P<0.0001

N-CELA3B (exocrine)

I

ND   T2D

INS   N-CELA3B

J   ND

N-CELA3B signal intensity (A.U./µm²)

K   T2D

N-CELA3B signal intensity (A.U./µm²)

L

kDa

ND HI   T2D HI   1 2 5 10 PE (ng)

35 -

CELA3B

M

Optical density (A.U.)

y = 1618.4x + 798.16
R² = 0.9915

PE (ng)

Samples	Amount (ng) of CELA3B per 1x10⁶ β-cells	Final concentration
ND HI	312.3 ± 170.6	~150 ng/ml
T2D HI	2183.7 ± 353.5	~1000 ng/ml

N

EdU⁺ cells (%)

P=0.0235
P<0.0001

PBS   PE 100 ng/ml   PE 500 ng/ml

O

Annexin V⁺ cells (%)

P<0.0001

P

sivelestat

Remaining activity (%)

Concentration (µM)

telaprevir

Remaining activity (%)

Concentration (µM)

tebipenem

Remaining activity (%)

Concentration (µM)

Figure S1. Expression levels of acinar, islet, ductal cells and neutrophil-specific genes, quantification of CELA3B amount in islets, and effects of HTS candidates on cathepsin G activity, Related to Figure 1 and 2.

(A-E) Transcript levels of (A) *CTSG* (B) *AMY2A*, (C) *PDX1,* (D) *KRT19*, and (E) *MUC1* in human endocrine and exocrine pancreatic cells from non-diabetic (ND) and type 2 diabetic (T2D) donors and bone marrow. N/d: non detected. Data are mean $\pm$ SEM. One-Way ANOVA test was used with Fisher's LSD correction for multiple comparisons.

(F) Testing of the affinity of antibodies against N-CELA3B (cleaved, cl) and CELA3B (full length, fl) forms using a recombinant human N-CELA3B (rhN-CELA3B) protein and human PE at different amounts (ng).

(G) Representative confocal imaging of CELA3A staining (magenta) in human pancreas from ND (left panel) and T2D (right panels) donors. Islets were labeled using insulin immunostaining (INS, green). Nuclei were stained using DAPI (blue). Scale bars are indicated within the pictures.

(H) Correlation plot between the cell area-normalized N-CELA3B intensity staining in the exocrine pancreas (X-axis) and islets (Y-axis) in sections from ND (pink dots) and T2D (green dots) donors. Shaded ovals indicate clusters of the two groups.

(I) Representative whole-section scans of the head region of pancreas from a non-diabetic (nPOD case #6535, left panel) and a Type 2 diabetic (nPOD case #6110, right panel) subject stained with N-CELA3B (red) and insulin (green). Numbers and solid lines identified different lobules across the section. Scale bars are 2mm.

(J and K) Expression levels of N-CELA3B in islets from lobules of pancreatic sections obtained from (O) non-diabetic donors (N=6) and (P) subjects with type 2 diabetes (N=7).

(L) Blot of CELA3B amounts in human islet samples with respect to a PE standard curve.

(M) CELA3B amount (ng) per 1×10^6 β-cells and concentration estimated in ND and T2D HI using a standard curve of PE from blot in L.

(N and O) Percentages (%) of (K) EdU$^+$ and (L) Annexin V$^+$ EndoC-βH3 cells at the indicated conditions. Data are mean $\pm$ SEM. One-Way ANOVA test was used with Fisher's LSD correction for multiple comparisons.

(P) Validation of sivelestat (green curve), telaprevir (red curve) and tebipenem (yellow curve) effect on human cathepsin G activity. Data are mean $\pm$ SEM.
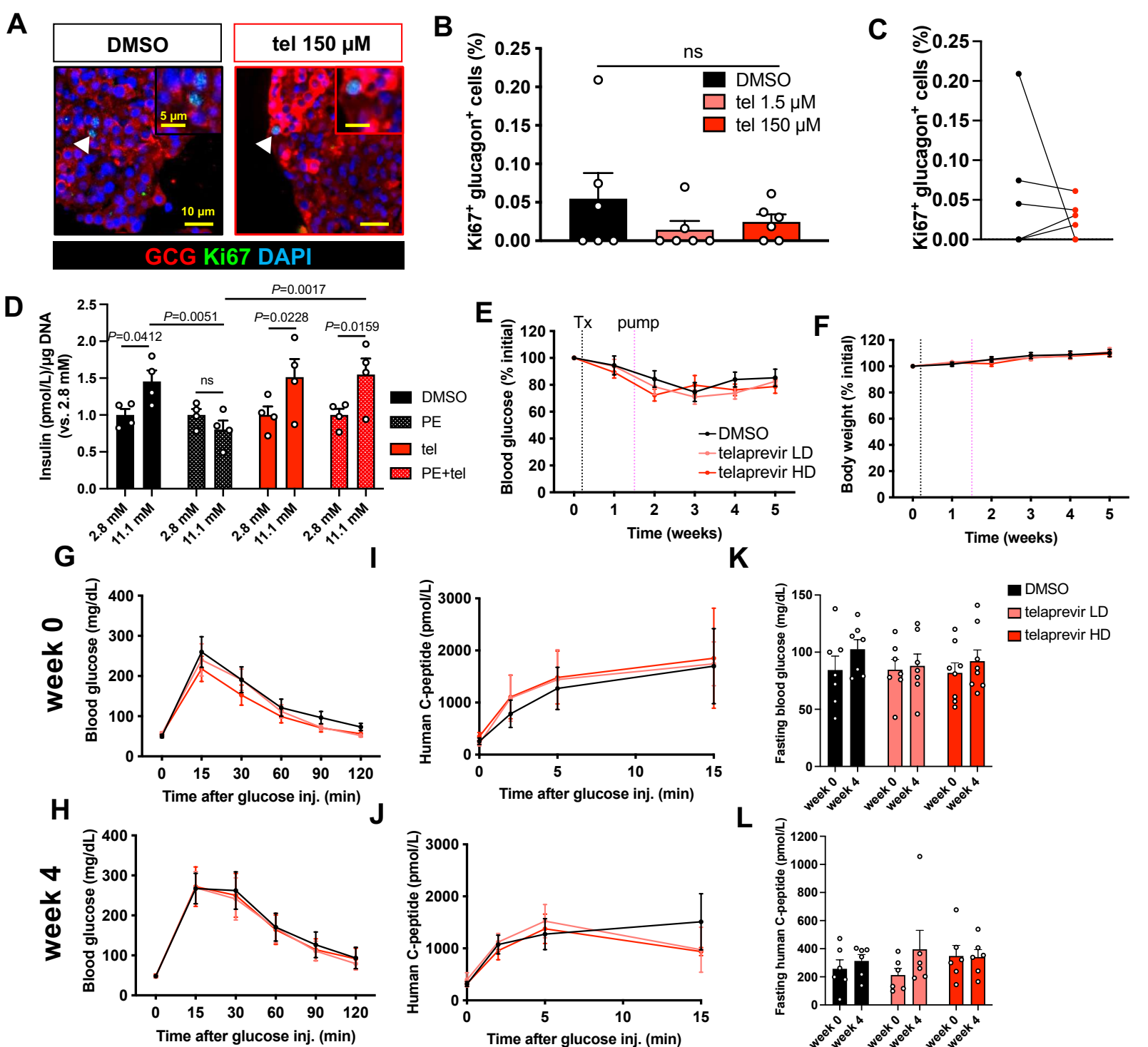
Figure S2. Effects of telaprevir on human α-cell proliferation and glucose homeostasis in humanized mouse models, Related to Figure 3.

(A) Representative picture of Ki67 (in green), glucagon (in red), and DAPI (in blue) labeling by immunohistochemistry in non-diabetic human islets treated with either DMSO (left panel) or telaprevir at 150 μM (right panel). Arrows indicate α-cells. Scale bars are indicated in the figure.

(B) Quantification of Ki67$^+$ glucagon$^+$ cell percentage in samples in A. Data are mean ± SEM. Paired One-Way ANOVA test was used with Fisher's LSD correction for multiple comparisons. Ns: non-significant.

(C) Paired analysis of Ki67$^+$ glucagon$^+$ cells extrapolated from graphs in B. Two-tailed paired t-test was used.

(D) Insulin release assays in EndoC-βH1 cells treated at the indicated conditions overnight. Data are mean ± SEM. Two-Way ANOVA test was used with Fisher's LSD correction for multiple comparisons. Ns: non-significant

(E and F) Curves of (E) random-fed blood glucose and (F) body weight excursions in transplanted NSG mice at the indicated conditions. Black dotted vertical lines indicate the time of human islet transplantations, whereas purple dotted line indicate the time of pump implantations. Data are mean of % initial values ± SEM.

(G-J) Curves of (G and H) glucose tolerance test and (I and J) serum human C-peptide levels following *in vivo* glucose-stimulated insulin secretion (GSIS) in humanized mice at week 0 (G and I) and week 4 (H and J) at the indicated conditions. Data are mean ± SEM.

(K and L) Fasting (K) blood glucose and (L) serum human C-peptide levels in transplanted mice measured at week 0 and week 4 at the indicated conditions. Data are mean ± SEM.
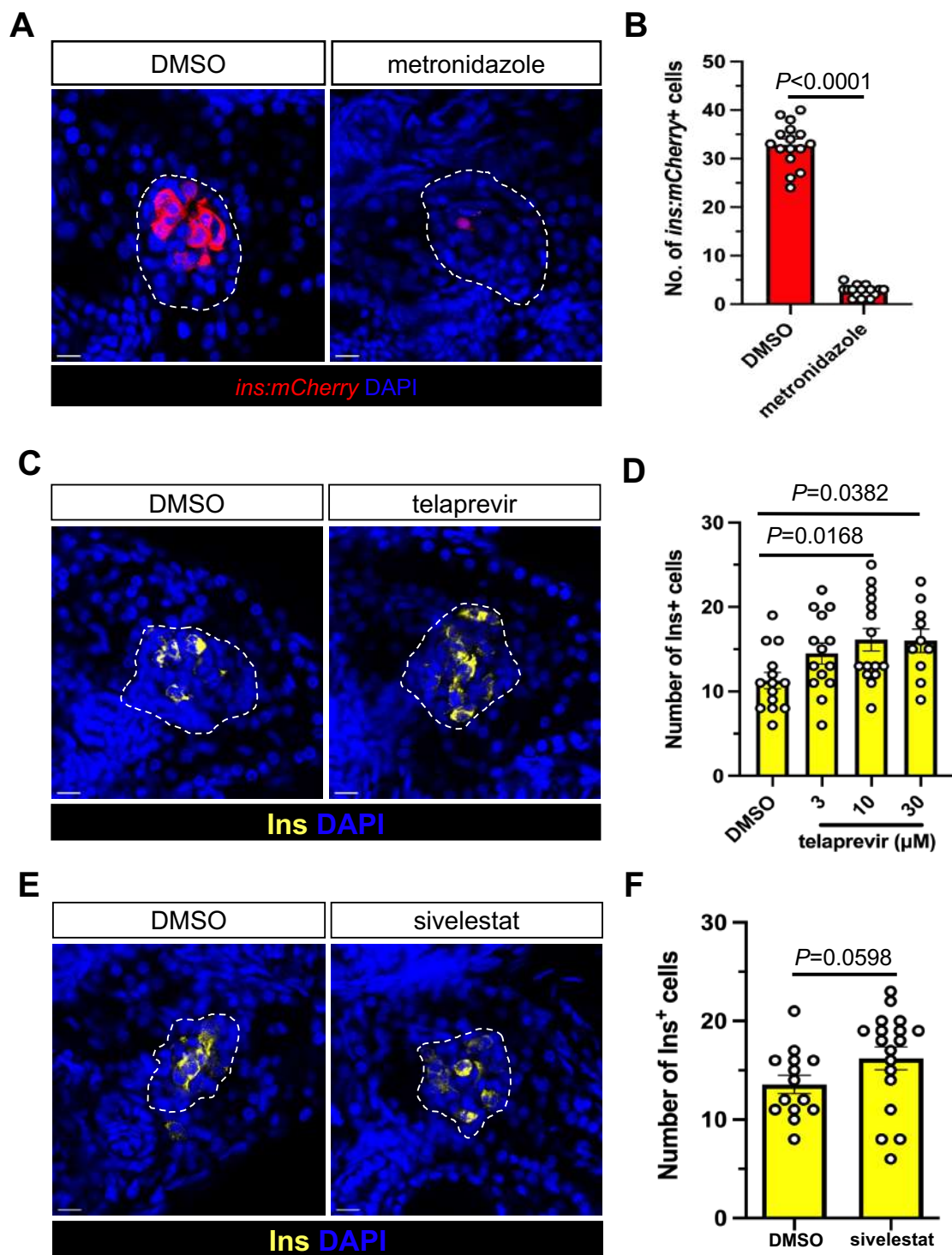
Figure S3. Effects of telaprevir on human β-cell function and β-cell numbers in zebrafish models of diabetes.
(A) Representative image of zebrafish pancreatic β-cells, labeled by the intrinsic expression of mCherry (red) before (left panel) and after (right panel) treatment with metronidazole at 3 dpf. Images were taken at 4 dpf. Nuclei are stained with DAPI (blue). Dotted lines mark the Ins+ cell clusters. Scale bar is 10 μm.
(B) Quantification of Ins:mCherry+ cells (Y-axis) in animals treated at the indicated conditions. Data are mean ± SEM (N=16). Unpaired two-tailed Student t-test was used to determine significance.
(C and E) Representative pictures of pancreatic islets of *Tg(ins:flag-NTR);Tg(tp1:H2BmCherry)* zebrafish larvae at 4-6 dpf treated with either DMSO (left panels) or (C) telaprevir (right panel) at the indicated concentrations or (E) sivelestat (right panel) at 10 μM concentration. Ins+ cells are labeled in yellow, and nuclei are stained with DAPI (blue). Dotted lines mark the Ins+ cell clusters. Scale bar is 10 μm.
(D and F) Quantification of Ins+ cells after treatments with (D) telaprevir or (F) sivelestat at the indicated concentrations. Data are mean ± SEM (N=10-18). One-way ANOVA test with Dunnett's correction for multiple comparisons (D) and unpaired two-tailed Student t-test were used.
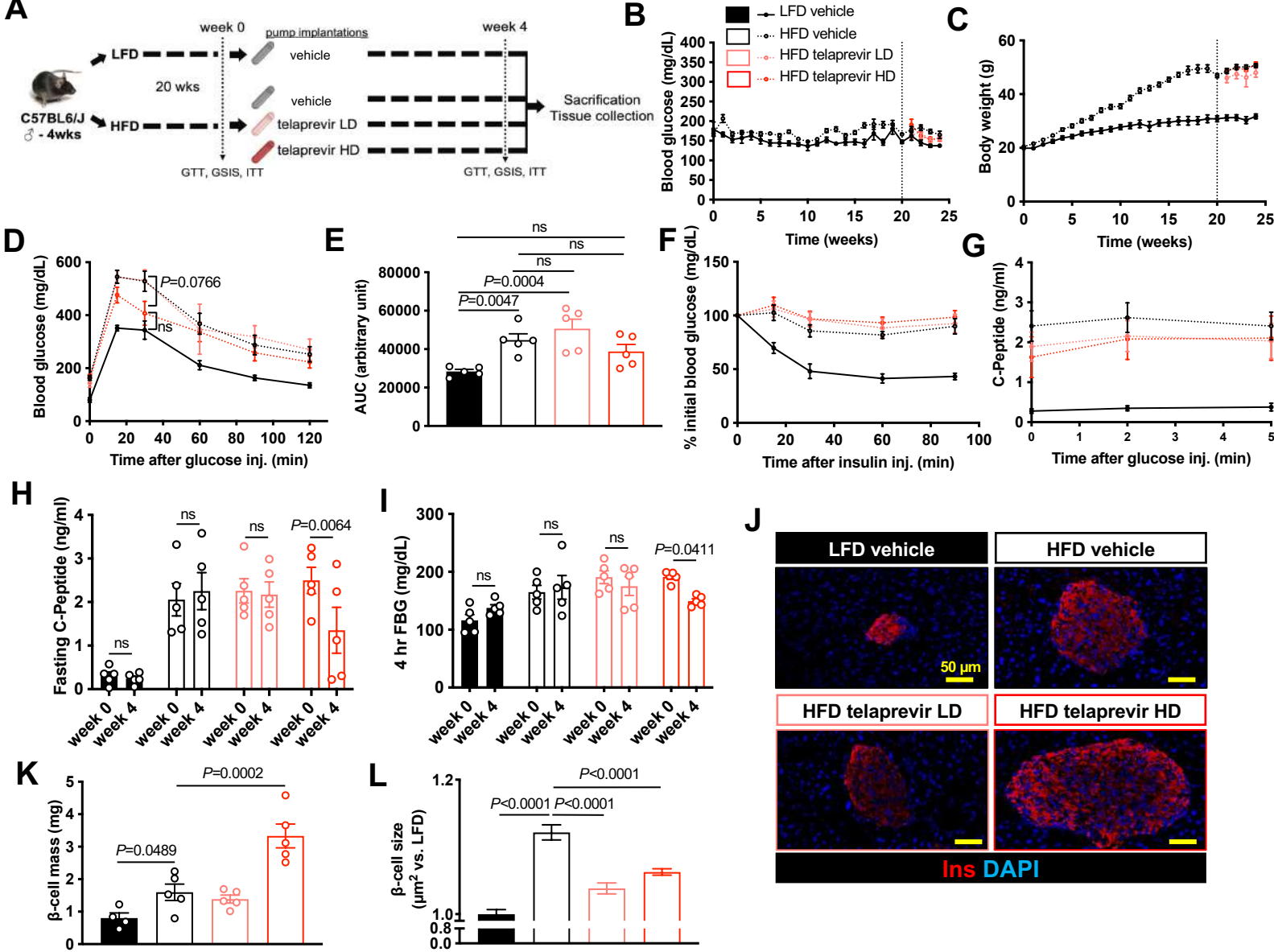
Figure S4. Effects of telaprevir on β-cell numbers and glucose homeostasis in zebrafish and mouse models of diabetes.

(A) Schematic design of the studies using HFD mouse models.

(B and C) Curves of (B) random-fed blood glucose and (C) body weight excursions in mice at the indicated treatments. Data in D are normalized on the initial body weight values. Black dotted vertical lines indicate the time of pump implantations. Data are mean ± SEM (N=5).

(D) Glucose tolerance test (GTT) curves in mice at the indicated conditions. Data are mean ± SEM. Two-way ANOVA test was used with Fisher's LSD correction for multiple comparisons.

(E) Area under the curve (AUC) of GTT curves in D. Data are mean ± SEM. One-way ANOVA test was used with Fisher's LSD correction for multiple comparisons.

(F) Insulin tolerance test (ITT) curves in mice at the indicated conditions. Data are means of normalized on the initial blood glucose levels ± SEM.

(G) Serum C-peptide levels following *in vivo* glucose-stimulated insulin secretion (GSIS) in mice at the indicated conditions. Data are mean ± SEM.

(H and I) Fasting (H) C-peptide and (I) blood glucose levels after (H) 16 h and (I) 4 h fasting in mice at the indicated conditions. Data are mean ± SEM. Two-way ANOVA test was used with Fisher's LSD correction for multiple comparisons.

(J) Representative pictures of insulin (in red) immunostaining in pancreatic sections from mice at the indicated conditions. Nuclei are stained with DAPI (in blue).

(K) Quantification of β-cell mass in pancreatic sections (n=2-3/mouse) from J. Data are mean ± SEM. One-way ANOVA test was used with Fisher's LSD correction for multiple comparisons.

(L) Quantification of β-cell size in mice treated at the indicated conditions. Data are mean of β-cell size expressed as fold change of the low-fat diet (LFD) values ± SEM. One-Way ANOVA test was used Fisher's LSD correction for multiple comparisons

Selected differentially regulated pathways (sivelestat vs. DMSO)

A 10 min

-log$_{10}$(FDR)

Pathway	Value
EGF-EGFR signaling pathway	11/162
PDGFR-β signaling pathway	7/127
Toll Like Receptor 7/8	5/79
VEGFA-VEGFR2 Signaling Pathway	13/433
VEGFA-VEGFR2 Pathway	7/92
Signaling by VEGF	7/100
Cell cycle	7/120
FOXM1 transcription factor network	5/42
Leptin signaling	6/76
Leptin	5/62
Hippo Signaling	6/98
Hippo signaling pathway	3/157
MAPK signaling pathway	8/294
MAPK3 activation	2/3
α6β4 signaling pathway	4/33
Focal adhesion	7/201
Insulin Pathway	4/46
IGF1 pathway	3/30

B 30 min

-log$_{10}$(FDR)

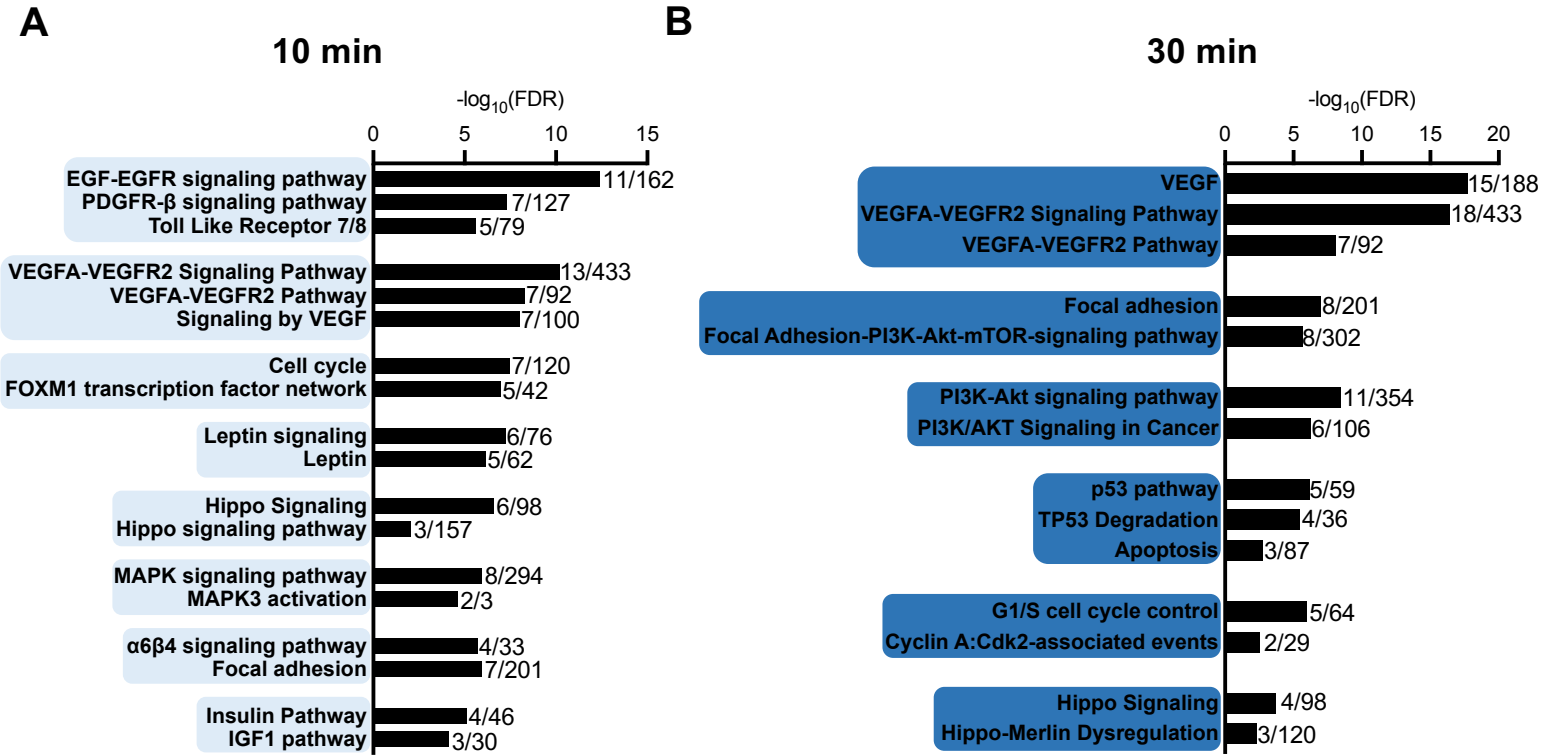| Pathway	Value
VEGF	15/188
VEGFA-VEGFR2 Signaling Pathway	18/433
VEGFA-VEGFR2 Pathway	7/92
Focal adhesion	8/201
Focal Adhesion-PI3K-Akt-mTOR-signaling pathway	8/302
PI3K-Akt signaling pathway	11/354
PI3K/AKT Signaling in Cancer	6/106
p53 pathway	5/59
TP53 Degradation	4/36
Apoptosis	3/87
G1/S cell cycle control	5/64
Cyclin A:Cdk2-associated events	2/29
Hippo Signaling	4/98
Hippo-Merlin Dysregulation	3/120

Figure S5. Short-term effects of sivelestat treatments on signaling pathways in human islets, Related to Figure 4.
(A and B) Selected differentially regulated pathways human islets treated with sivelestat for (A) 10 min or (B) 30 min.
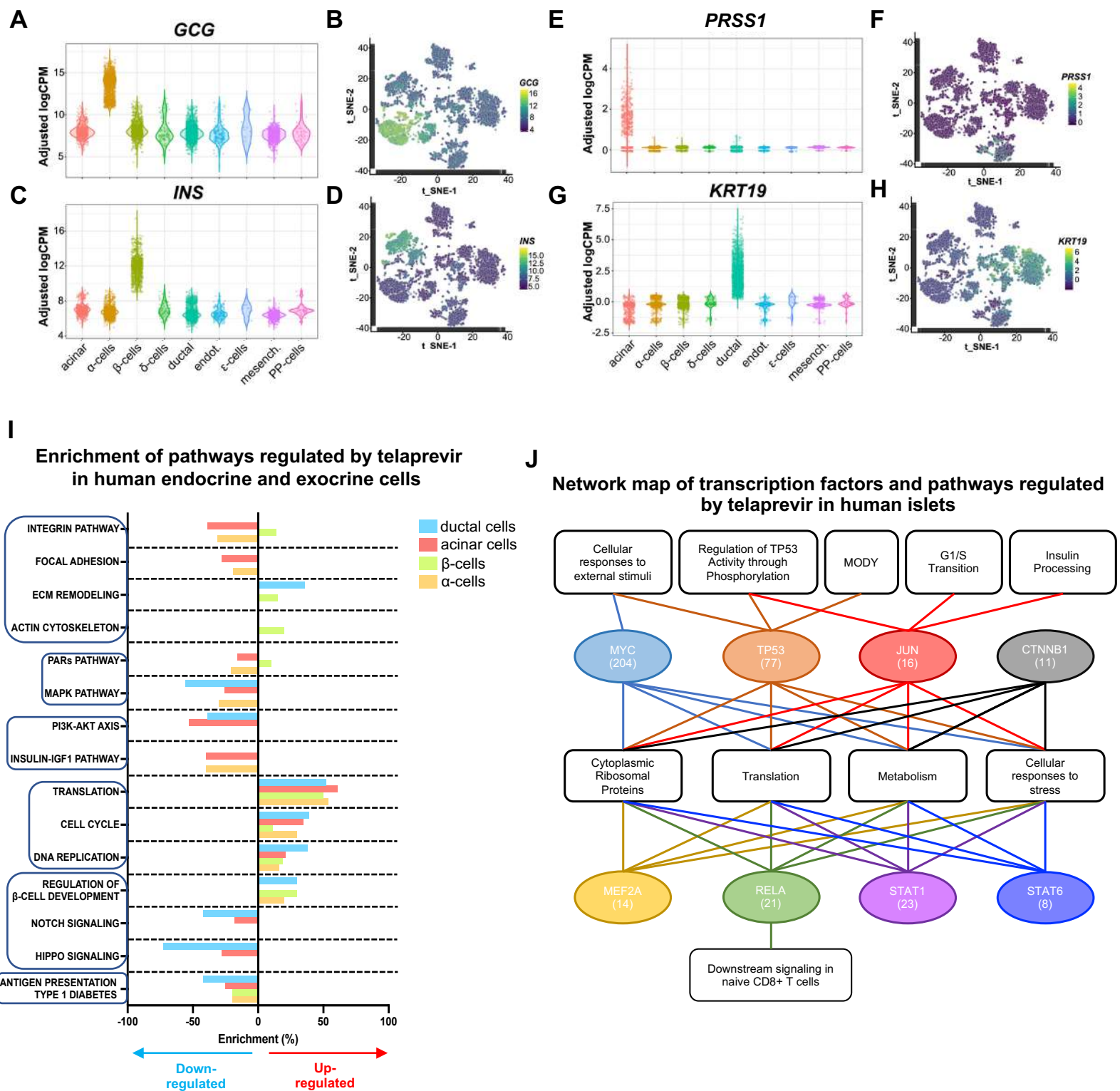
Figure S6. Expression levels of α-cell, β-cell, acinar cell and ductal cell marker genes and telaprevir-regulated pathways in human endocrine and exocrine cells, Related to Figure 5.

(A, C, E and G) Violin plots of (A) *GCG*, (C) *INS*, (E) *PRSS1*, and (G) *KRT19* transcript levels in the indicated cell clusters from the scRNA-seq. Expression levels are reported as adjusted log count per millions (CPM, Y-axis).

(B, D, F and H) Expression levels of (B) *GCG*, (D) *INS*, (F) *PRSS1*, and (H) *KRT19* genes within the global cell distribution t_SNE plots, ranging from high (yellow-green) to low (purple) levels.

(I) Directionality of the indicated pathways in the indicated cell types from human islets treated with telaprevir vs. DMSO-treated samples. Data are plotted as percentage of enrichment of differentially regulated genes in each pathway.

(J) Interconnections between transcription factors (circles) and pathways (squares) differentially regulated in human islets and β-cells by telaprevir, respectively.
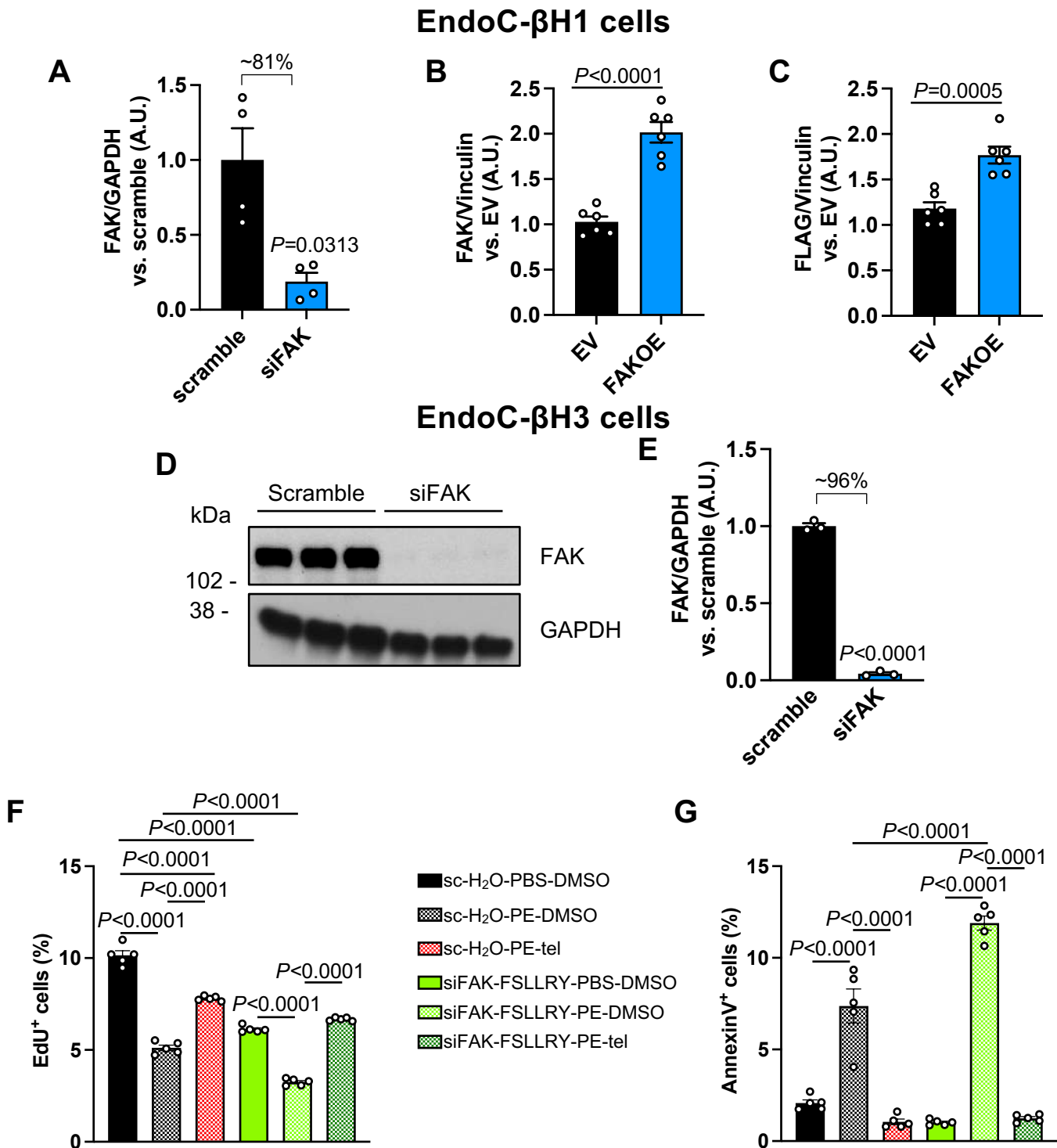
Figure S7. Efficiency of FAK silencing and overexpression and proliferation and apoptosis levels in EndoC-βH1/3 cells following blockade of mechano-signaling and PAR2 pathways, Related to Figure 7.
(A) Quantification of FAK protein levels in EndoC-βH1 samples showed in Figure 7B,C following FAK knock-down. Data mean ± SEM. Two-tailed unpaired t-test was used.
(B and C) Quantification of (B) FAK and (C) FLAG protein levels in EndoC-βH1 samples showed in Figure 7D,E following FAK overexpression. Data mean ± SEM. Two-tailed unpaired t-test was used.
(D) Representative blots of FAK and GAPDH protein levels in scramble and siFAK EndoC-βH3 cells.
(E) Quantification of FAK protein levels normalized on GAPDH protein levels from B. Data are mean ± SEM. Two-tailed unpaired t-test. was used.
(F and G) Percentages (%) of (F) EdU+ and (G) Annexin V+ EndoC-βH3 cells at the indicated conditions. Data are mean ± SEM. One-Way ANOVA test was used with Fisher's LSD correction for multiple comparisons.

Table S1. Characteristics of donors of human pancreas, islet and acinar cell samples. Related to Figure 1, 3, 4, 5, 6, and Figure S1, S2, S5 and S6. ND: non-diabetic; T2D: type 2 diabetes; nPOD: network for Pancreatic Organ Donors with Diabetes; BMI: body mass index.

Human pancreas							
Disease state	nPOD ID	Age (y)	Gender	Ethnicity	BMI (kg/m^2)	C-Peptide (pmol/L)	Duration of T2D (y)
Non-diabetic (ND)	6009	45	M	Caucasian	30.6	11.32	N/A
	6034	32	F	Caucasian	25.2	3.15	N/A
	6168	51	M	Hispanic	25.2	N/A	N/A
	6331	27	F	African American	24.0	3.01	N/A
	6487	27	M	African American	27.8	5.52	N/A
	6535	31	F	Caucasian	29.6	6.59	N/A
Type 2 diabetic (T2D)	6110	20.7	F	African American	40	0.58	N/D
	6133	46	F	Caucasian	40.2	0.84	20
	6194	47	M	Caucasian	23.7	0.16	13
	6221	61	F	Caucasian	33.7	3.05	4
	6277	48	M	African American	29.5	0.47	10
	6329	49	F	Hispanic	36.4	7.46	25
	6541	57	M	Hispanic	26.9	3.41	1

HbA1c: glycated hemoglobin.

Human islets									
Application	Disease state	RIID or Prodo ID	Age (y)	Gender	Ethnicity	BMI (kg/m^2)	HbA1c (%)	Purity (%)	Viability (%)
RT-PCR	ND	SAMN08612554	51	F	Hispanic	32	5.3	90	90
		SAMN08619388	60	F	African American	18.2	6.0	80	87
		SAMN08930760	45	M	Caucasian	30.5	5.0	90	96
		SAMN08769124	15	M	Hispanic	24.6	5.1	80	97
		SAMN0876908	49	M	Caucasian	26.3	5.1	95	95
	T2D	HP-18165-01T2D	63	M	Hispanic	22	7.3	85	95
		SAMN10832912	54	M	African American	33.7	8.0	90	94
		SAMN11245238	66	F	Caucasian	29.8	6.5	90	95
		SAMN08769092	57	M	Hispanic	34.6	10.4	98	80
		SAMN08930811	47	M	Caucasian	32.2	5.7	70	63
		SAMN08933946	52	M	Caucasian	50.0	N/A	92	99
		SAMN08786217	49	M	N/A	28.2	N/A	90	95
		SAMN08769072	55	M	Caucasian	32.5	14.7	96	73
WB	ND	SAMN08611211	45	M	Caucasian	29.8	5.1	95	95
		SAMN08619527	28	M	Caucasian	34.7	4.2	95	95
		SAMN15942269	63	F	African American	26.9	5.5	80	98
		SAMN13972304	49	M	Latino	34.8	5.5	90	96
		HP-17036-01	59	M	Caucasian	26.9	5.8	90	90
		HP-20199-01	21	M	Hispanic	27.3	5.3	90	95
	T2D	HP-18103-01T2D	35	F	Hispanic	34	7.1	85	95
		SAMN09498258	54	M	Hispanic	23.6	5.8	83	96
		SAMN11157311	34	F	Caucasian	31.7	7.3	92	92
		SAMN08786337	53	M	N/A	31	N/A	60	96
		SAMN08769092			See above				
		SAMN08768765	65	F	Caucasian	42.6	5.9	95	95
IHC	ND	SAMN08768991	51	M	Caucasian	29	5.1	85	95
		SAMN08611141	48	M	Hispanic	32.4	5.6	95	95
		SAMN08611143	32	M	Caucasian	26.2	5.3	85	98
		HP-18054-01	40	M	Hispanic	25	5.3	95	95
		HP-18304-01	21	M	Hispanic	27.3	5.4	85	95

Application	Disease state	Prodo ID	Age (y)	Gender	Ethnicity	BMI	HbA1c		
		HP-18310-01	38	M	Hispanic	28	5.9	90	95
Transplantations	ND	SAMN12227196	51	M	Caucasian	32.8	4.9	95	95
		HP-19226-01	51	M	Caucasian	31.3	5.2	95	95
		HP-19073-01	50	M	Caucasian	21.2	5.5	90	95
		SAMN13836615	58	M	Hispanic	23.2	5.7	90	95
		HP-20030-01	67	M	Hispanic	22.5	5.5	90	95
		HP-20191-01	39	F	Caucasian	21.9	5.6	95	95
		HP-20199-01	21	M	Hispanic	27.3	5.1	95	95
Phospho-antibody microarrays	ND	SAMN09768368	56	F	Caucasian	26.6	N/A	90	90
		HP-18336-01	61	F	Caucasian	24.5	5.1	90	95
		HP-18341-01	48	M	Caucasian	26.3	5.1	90	95
scRNA-seq	ND	SAMN10079665	25	M	Caucasian	31	5.0	95	98
		HP-19073-01				*See above*			
		HP-19102-01	40	F	Hispanic	31.8	4.8	95	95
WB (signaling pathways)	ND	HP-19283-01	43	F	Caucasian	31.7	5.7	90	95
		HP-18196-01	49	M	Hispanic	30.3	5.8	85	95
		SAMN13186657	44	F	Hispanic	24.1	5.8	90	95
		SAMN09768368	56	F	Caucasian	26.6	N/A	90	90
		SAMN09228907	62	M	African American	36.1	5.8	90	95
Viability assays following PAR2 inhibition	ND	HP-21132-01	31	M	Caucasian	26.6	5.2	90	95
		HP-21146-01	39	M	Caucasian	27.6	5.5	85	95
		HP-21148-01	19	M	N/A	23.1	5.8	95	95
		HP-21161-01	43	M	Hispanic	25.5	5.4	90	95

Human acinar cells							
Application	**Disease state**	**Prodo ID**	**Age (y)**	**Gender**	**Ethnicity**	**BMI (kg/m²)**	**HbA1c (%)**
RT-PCR	ND	HP-18336-01			*See above*		
		HP-18132-01	45	M	Hispanic	25	5.1
		HP-18144-01	47	M	N/A	28.1	5.8
	T2D	HP-18165-01T2D			*See above*		
		HP-18179-01T2D	59	F	Asian	34	6.7
		HP-20259-01T2D	59	M	Hispanic	25.1	7.3
WB	ND	HP-20268-01	55	M	Hispanic	23	4.7
		HP-19030-01	25	M	Hispanic	27.3	5.2
		HP-18132-01			*See above*		
		HP-17346-01	27	M	Native American	25.8	5.6
	T2D	HP-18179-01T2D			*See above*		
		HP-18320-01T2D	61	M	African American	27.4	7.1
		HP-18165-01T2D			*See above*		
		HP-20259-01T2D	59	M	Hispanic	25.1	7.3

Table S2: List of oligonucleotides used for gene expression analysis. Related to Figure 1 and Figure S1.

Gene name	Accession number	Forward sequence (5'-3')	Reverse sequence (5'-3')
ELANE	NM_001972.4	TGCGCCCAACTTCGTCATGTCG	CGTAGCCGTTTTCGAAGATGCG
CELA2A	NM_007919.2	GCACAAGGACTGGAACTCCAAC	GTTGTTGGGTAGAATGGTGCCG
CELA2B	NM_015849.3	GCCAGCATAACCTCTACGTTGC	GCCAGTTTGAGCAGGGCAATGT
CELA3A	NM_005747.5	GCTGGTGACATCCTTCCCAACA	AGTTCCACCTGGAGCAGTGCTT
CELA3B	NM_007352.3	CTGGTGACATCCTTCCCAACGA	GGAGCAGTGTTCATAGTCCACC
AMY2A	NM_000699.4	GATAATGGGAGCAACCAAGTGGC	CAGTATGTGCCAGCAGGAAGAC
PDX1	NM_000209.4	GAAGTCTACCAAAGCTCACGCG	GGAACTCCTTCTCCAGCTCTAG
CTSG	NM_001911.3	ACACCCAGCAACACATCACTGC	GGTTCACGTTTCGATTCCGTCTG
ACTB	NM_001101.3	CACCATTGGCAATGAGCGGTTC	AGGTCTTTGCGGATGTCCACGT

Table S3: Numbers of high-quality recovered cells from scRNA-seq experiments, Related to Figure 5.

	α-cells	β-cells	PP-cells	δ-cells	ε-cells	acinar cells	ductal cells	endothelial cells	mesenchymal cells	Total
DMSO	214	157	8	17	2	222	430	58	91	1199
Telaprevir	619	456	18	48	11	269	1269	100	404	3194
Sivelestat	469	338	12	33	4	89	459	40	212	1656

Table S4: Genes linked to cytoskeleton remodeling pathway regulated by the indicated transcription factors in human beta-cell treated with telaprevir, Related to Figure 5.

Gene symbol	Description	TF	FC	FDR
ANXA2	Annexin A2	CTNNB1, TP53	1.28	0.00973
DSP	Desmoplakin	CTNNB1, TP53	1.26	0.00841
BRK1	BRICK1 subunit of SCAR/WAVE actin nucleating complex	MYC	1.27	1.41E-05
ACTG1	Actin gamma 1	MYC	1.26	0.00532
ARPC1B	Actin related protein 2/3 complex subunit 1B	MYC, STAT1	1.33	0.000284
DSTN	Destrin	MYC, RELA, TP53	1.4	2.77E-16
LGALS1	Galectin 1	RELA	1.45	1.81E-08
VIM	Vimentin	RELA, TP53	1.35	0.00697